

Effect of NO, CO, and Cl₂ on Mixed-Mode Regimes in the Belousov–Zhabotinsky Oscillating Chemical Reaction in a CSTR

Peter E. Strizhak,^{*,†} Vyacheslav O. Khavrus,[†] and Kedma Bar-Eli^{‡,§}

L.V. Pysarzhevsky Institute of Physical Chemistry of the National Academy of Sciences of Ukraine, pr. Nauki 31, Kiev, 03039, Ukraine, and Tel-Aviv University, Raymond and Beverly Sackler Faculty of Exact Sciences, School of Chemistry, Tel-Aviv, 69978, Israel

Received: May 9, 2001; In Final Form: December 18, 2001

We have studied the effect of gases (NO, CO, Cl₂) on mixed-mode regimes in the Belousov–Zhabotinsky oscillating chemical reaction in a CSTR. Mixed-mode regimes are characterized by a single large-amplitude oscillation followed by a number of small-amplitude oscillations. Bubbling of the gas into the inflow solution changes the average number of small-amplitude oscillations. We show that the average number of small-amplitude oscillations depends linearly on the gas concentration. A good agreement between the experimental data and simulations with the Györgyi–Field model is obtained.

1. Introduction

The Belousov–Zhabotinsky (BZ) oscillating chemical reaction exhibits a variety of dynamic regimes, such as bistability, periodic oscillations, mixed-mode oscillations, chaotic dynamics, etc.^{1–10} All these regimes have been found in the BZ reaction catalyzed by cerium as well as by ferroin.^{19,11,12} Recently we have shown that the BZ reaction catalyzed by ferroin exhibits various mixed-mode regimes.⁹ They consist of a single large-amplitude oscillation (L) followed by a number (*n*) of small-amplitude oscillations (S). The symbol LS^{*n*} is conveniently attributed to these regions.

Mixed-mode regimes and chaotic behavior in oscillating chemical reactions may be drastically affected either by impurities of reagents or by injection of small amounts of various chemical compounds.^{11,13,14} Impurities may change the complex dynamics of the oscillating reaction.^{11,13–15} In particular the oscillations pattern may change even as small amounts of perturbing species are present.^{13–14}

In this paper we present a study of an effect of NO, CO, or Cl₂ on mixed-mode regimes in the BZ reaction catalyzed by ferroin in a continuously flow stirred tank reactor (CSTR). We show that bubbling of NO, CO, or Cl₂ into the inflow solution changes the number of small-amplitude oscillations in mixed-mode regimes. The number of small-amplitude oscillations depends linearly on the gas concentration. An explanation of these experimental observations is given using the Györgyi–Field model of the BZ reaction.¹⁶ We show that by adding feasible chemical reactions of these gases with the species involved in the mechanism, a good agreement between the simulations and experimental results is obtained.

2. Experimental Section

All reagents were analytical grade. Stock solutions of 0.3 M KBrO₃, 4 M malonic acid (MA), 6 M H₂SO₄, and 2.5 × 10⁻²

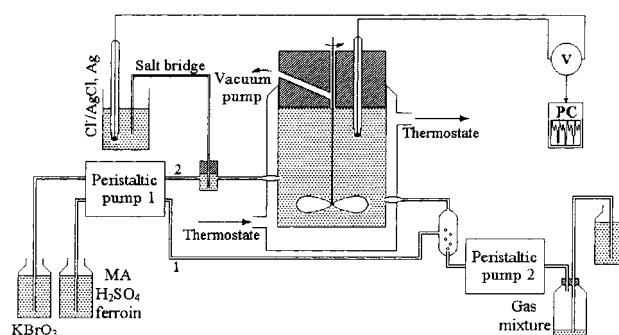


Figure 1. Schematic diagram of the experimental setup.

M ferroin were prepared using double distilled water. Gas mixtures of each gas with argon were prepared volumetrically. The total pressure of gas mixture was 101 kPa. Details of experimental setup have been published recently.¹⁵

All studies were conducted using the experimental setup shown schematically in Figure 1. The continuously stirred flow tank reactor (CSTR), inflow solutions, and examined gas mixture were thermostated at the constant temperature $T = 295.5 \pm 0.1$ K. Stirring rate was 1000 ± 30 rpm in all the experiments. The state of the system was monitored by measuring the platinum electrode potential using a silver/silver chloride electrode as a reference. The impedance-matched electrode signals were fed via a Data Translation A/D converter board into a personal computer. Signals were recorded as a function of time with time step 0.1 s. The Pt electrode potential corresponding to asymptotic oscillating mixed-mode regime was recorded after transient regime (not less than 1500 s). The mixed-mode regimes are not caused by any effect of a peristaltic pump because there is no correlation between pulsation of the peristaltic pump and time intervals between either small- or large-amplitude oscillations. We have also checked that the mixed-mode regimes exist in a wide range of stirring rates. All experiments were performed at a constant stirring rate, so all differences can be safely attributed to the addition of the gases.

Reagents were flowed into the reactor by a peristaltic pump through two channels. Solution 1 containing 0.48 M malonic acid, 0.64 M H₂SO₄, and 3.4 × 10⁻³ M ferroin was pumped

* Corresponding author. E-mail: pstrizhak@hotmail.com.

[†] L.V. Pysarzhevsky Institute of Physical Chemistry of the National Academy of Sciences of Ukraine.

[‡] Tel-Aviv University.

[§] E-mail: kedma@ccsg.tau.ac.il.

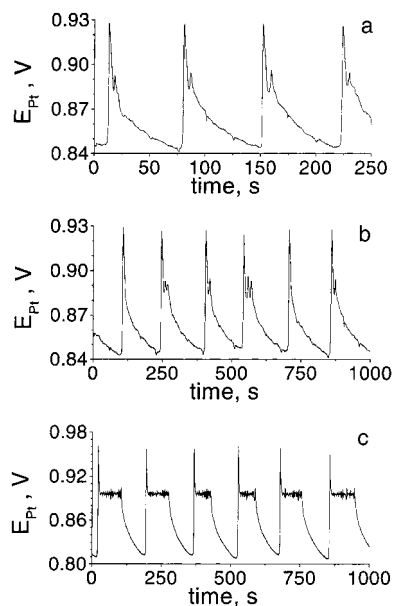


Figure 2. Time dependencies of Pt-electrode potential at different flow rates: 0.00187 s⁻¹ (a), 0.00208 s⁻¹ (b), 0.00555 s⁻¹ (c) ($T = 295.5$ K; $[\text{KBrO}_3]_0 = 0.15$ M; $[\text{H}_2\text{SO}_4]_0 = 0.32$ M; $[\text{MA}]_0 = 0.24$ M; $[\text{ferroin}]_0 = 1.7 \times 10^{-3}$ M).

through the first channel, and solution 2 of 0.3 M KBrO_3 was pumped through the second channel. Both stock solutions were saturated by argon. Known volumes of gas and argon were mixed before the experiment and the mixture was put in the aspirator at the lower right of Figure 1. The gas mixture was pumped by a separate peristaltic pump at a constant rate of 0.35 ± 0.01 mL/min into the reaction chamber. To keep the pressure constant, another aspirator was placed above the first one to replace by water solution the volume of gas spent. The constant flow of the gas mixture into the reaction chamber keeps the latter saturated with this mixture.

Our chromatography studies have indicated that the purity of the gases was not worse than 99% (vol/vol). Particularly, the oxygen concentration in the gas mixture did not exceed 0.001% (vol/vol).

3. Experimental Results

Depending on the flow rate (k_0), the BZ reaction exhibits different mixed-mode oscillations. Some of them are shown in Figure 2. At low flow rates the LS^1 pattern is shown in Figure 2a. As the flow rate increases, a pattern involving a mixture of LS^0 , LS^1 , and LS^2 is shown in Figure 2b. This develops further into Figure 2c, showing LS^n patterns with $n = 11-20$. Since the oscillations are not exactly periodic we have characterized the time series by the average number of the small-amplitude oscillations per single large-amplitude oscillation:

$$N = \frac{\text{number of small-amplitude oscillations/}}{\text{number of large-amplitude oscillations}}$$

The average number of small-amplitude oscillations N has been calculated for each time series lasting for at least 3 h and containing no less than 30 large-amplitude maxima. In each experiment the length of the time series was long enough to calculate the value of N with standard deviation less than 10% calculated for a single time series.

The first two columns of Table 1 show the dependence of N on k_0 if only pure argon is bubbled. It is seen that the average number of small-amplitude oscillations increases with k_0 . As any of the gases NO, CO, or Cl_2 is bubbled into the solution,

TABLE 1: Dependencies of Average Numbers of Small Amplitude Oscillations (N) under Argon and Values of π (slope of ΔN on the gas concentration) on Flow Rate (conditions are the same as in Figure 2)

k_0, s^{-1}	N	NO $\pi, 10^2 \text{ vol/vol}$	CO $\pi, 10^2 \text{ vol/vol}$	Cl_2 $\pi, 10^2 \text{ vol/vol}$
0.00208	1.5	-1.1	2.9	85.1
0.00267	4.6	-2.2	4.6	38.3
0.00340	7.5	-3.6	4.4	13.6
0.00435	13.1	-5.0	3.9	9.4
0.00555	17.6	-7.8	8.5	5.3
0.00710	29.8	-11.9	8.3	-8.5
0.00907	51.3	-25.1	20.9	-2.8

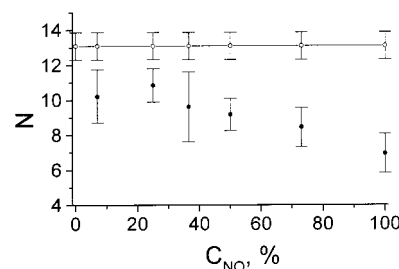


Figure 3. Dependencies of N on volume/volume percent of NO (closed circles) together with values of N for pure argon (a, open circles connected by line). Conditions are the same as in Figure 2, $k_0 = 0.00435 \text{ s}^{-1}$.

the value of N is changed depending on the gas and its concentration. The effect is more pronounced at high flow rates, i.e., for mixed-mode oscillations that are characterized by large numbers of small-amplitude oscillations. The effect is quantified by the difference between the average number of small oscillations, N , when pure argon or gas-argon mixtures are bubbled:

$$\Delta N(\text{gas}) = N(\text{gas}) - N(\text{Ar})$$

where $N(\text{gas})$ gives the average number of small-amplitude oscillations for a given gas concentration in its mixture with Ar, and $N(\text{Ar})$ is the corresponding number if pure argon is bubbled. Figure 3 shows the values of N (together with its error bars) vs the gas (NO) concentration (full circles) and also that of pure Ar (open circles). The difference between $N(\text{NO})$ and $N(\text{Ar})$ is clearly seen and thus the definition of $\Delta N(\text{gas})$ seems quite reliable.

Typical dependencies of $\Delta N(\text{gas})$ on gas concentrations are shown in Figure 4. In all cases they may be described by the following linear equation:

$$\Delta N(\text{gas}) = \alpha + \pi \times P_{\text{gas}}$$

where P_{gas} is the volume/volume percent of the gas in its mixture with argon.

In Figure 4 we see that NO causes a decrease in the average number of small oscillations, while CO causes an increase. The case of chlorine is intermediate, for small flow rate it increases, while for large ones it decreases. The values of π for NO, CO, and Cl_2 are presented in Table 1 for different flow rates. The slope decreases slightly with the flow rate for the case of NO, increases slightly for the case of CO, and decreases significantly for the case of Cl_2 and even goes negative at high flow rates.

4. Model

Mixed-mode oscillations similar to those obtained in experiments described above, may be obtained using the 4-variable model of the BZ reaction suggested by Györgyi and Field^{16,17}

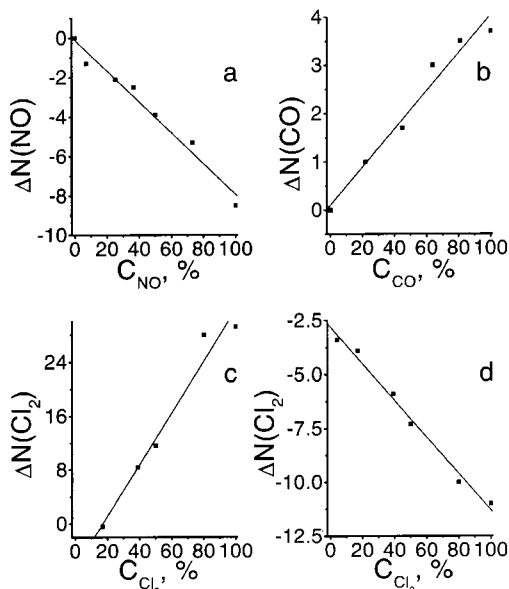


Figure 4. Dependencies of ΔN on volume/volume percents of different gases in their mixtures with Ar at different flow rates (conditions are the same as in Figure 2): (a) for NO at $k_0 = 0.00555 \text{ s}^{-1}$; (b) for CO at $k_0 = 0.00435 \text{ s}^{-1}$; (c) for Cl_2 at $k_0 = 0.00267 \text{ s}^{-1}$; (d) for Cl_2 at $k_0 = 0.00710 \text{ s}^{-1}$.

TABLE 2: Chemical Scheme for the 4-Variable Model of the BZ Reaction^{16,17,a,b,c}

	kinetic model ^b	rate constants ^a
(GF1)	$\text{BrO}_3^- + \text{Br}^- + 2\text{H}^+ \rightarrow \text{HBrO}_2 + \text{BrMA}$	$k_1 = 2.0 \text{ M}^{-3} \text{ s}^{-1}$
(GF2)	$\text{HBrO}_2 + \text{Br}^- + \text{H}^+ \rightarrow 2\text{BrMA}$	$k_2 = 2.0 \times 10^6 \text{ M}^{-2} \text{ s}^{-1}$
(GF3)	$\text{BrO}_3^- + (1/2)\text{HBrO}_2 + \text{H}^+ \rightleftharpoons \text{HBrO}_2 + \text{M}_{\text{ox}}$	$k_3 = 6.2 \times 10^4 \text{ M}^{-2} \text{ s}^{-1}$ ^b
(GF4)	$2\text{HBrO}_2 \rightarrow \text{BrO}_3^- + \text{BrMA}$	$k_3^- = 7000.0 \text{ M}^{-1} \text{ s}^{-1}$
(GF5)	$\text{M}_{\text{ox}} + \text{MA} \rightarrow$	$k_4 = 3000.0 \text{ M}^{-1} \text{ s}^{-1}$
(GF6)	$\text{BrMA} + \text{M}_{\text{ox}} \rightarrow \text{Br}^-$	$k_5 = 0.3 \text{ M}^{-1} \text{ s}^{-1}$
(GF7)	$\text{BrMA} \rightarrow \text{Br}^-$	$k_6 = 30.0 \text{ M}^{-1} \text{ s}^{-1}$
		$k_7 = 2.4 \times 10^4 \text{ M}^{-1} \text{ s}^{-1}$ ^e

^a Ref 16. ^b Ref 17. ^c The concentrations of BrO_3^- , MA, and H^+ are fixed: $[\text{KBrO}_3]_0 = 0.14 \text{ M}$; $[\text{MA}]_0 = 0.3 \text{ M}$; $[\text{H}^+] = 0.26 \text{ M}$; total concentration of the catalyst is $[\text{M}]_{\text{tot}} = 0.001 \text{ M}$. The rates of reactions GF1, GF2, and GF4–GF6 are defined by corresponding mass laws. ^d Rate of this reaction is defined as $v_3 = k_3 \times [\text{H}^+] \times ([\text{M}]_{\text{tot}} - [\text{M}_{\text{ox}}]) \times [\text{BrO}_2^*]$, where $[\text{BrO}_2^*] = (7.9 \times 10^{-7} \times [\text{BrO}_3^-] \times [\text{H}^+] \times [\text{HBrO}_2])^{1/2}$. ^e Rate of this reaction is defined as $v_7 = k_7 \times [\text{BrMA}] \times [\text{MA}^*]$, where $[\text{MA}^*] = [-k_7 \times [\text{HBrO}_2] + \{(k_7 \times [\text{HBrO}_2])^2 + 2.4 \times 10^{10} \times k_5 \times [\text{MA}] \times [\text{M}_{\text{ox}}]\}^{1/2} / (1.2 \times 10^{10})]$.

presented in Table 2. The scheme involves the four variables HBrO_2 , Br^- , BrMA , and ferriin (M_{ox}).^{16–19} Other species appearing in Table 2 are considered to be constant. In the Györgyi–Field (GF) model autocatalysis appears as the step GF3, limited by step GF4. Accumulation of bromomalonic acid is represented by steps GF1, GF2, and GF4. The steps GF1–GF4 correspond to reactions of an inorganic subset and provide for reactions of HBrO_2 governed by concentration of Br^- . Reactions of Br^- accumulation are presented by steps GF6–GF7.

The equations derived from the scheme of Table 2 (including terms for outflow of the reactants) were integrated numerically. Depending on the flow rate the model exhibits various mixed-mode oscillations, as seen in Figure 5, in qualitative similarity to those obtained experimentally and shown in Figure 2. In both cases the number N of the average small-to-large oscillations increases with the flow rate. The similarity between the experimental and calculated patterns is, of course, only qualita-

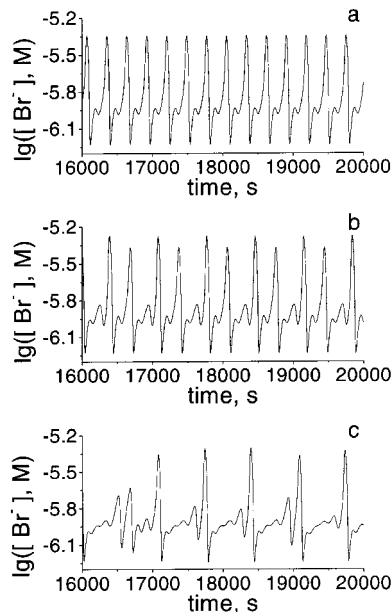


Figure 5. Time series for the bromide ion concentration obtained in simulations using the model presented in Table 2 at different flow rates: (a) $k_0 = 1.25\text{e-}3 \text{ s}^{-1}$; (b) $k_0 = 1.265\text{e-}3 \text{ s}^{-1}$; (c) $k_0 = 1.3109\text{e-}3 \text{ s}^{-1}$.

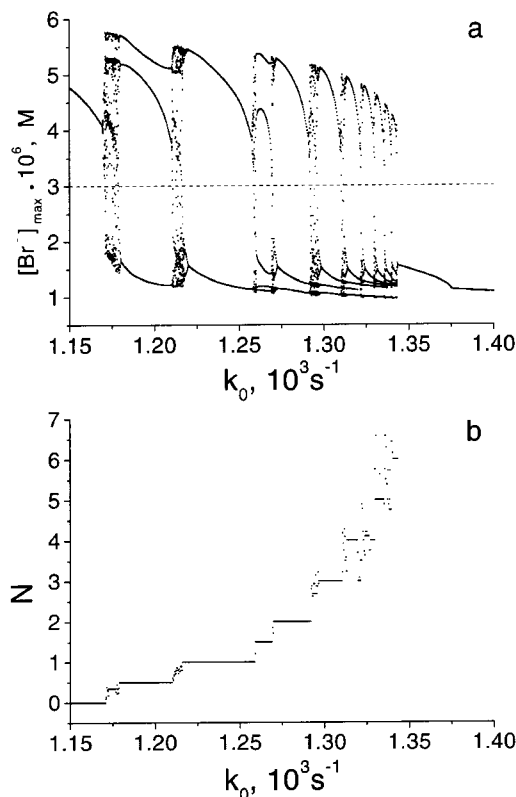


Figure 6. Bifurcation diagram (a) and dependence of N on k_0 (b) obtained in simulations according to the model presented in Table 2. Shown in panel (a) dashed line indicates our assumption that large-amplitude oscillations are attributed for the points above dashed line, whereas low-amplitude oscillations are attributed for the points below it.

tive as one does not expect to obtain a quantitative agreement between the simple GF model and the real experiment.

Figure 6a gives the bifurcation diagram constructed as the dependence of the maxima of bromide ions concentration on the flow rate. At low values of k_0 single large-amplitude oscillations exist. An increase of k_0 causes a sequence of period

adding bifurcations broken by chaotic behavior.^{20–24} At high values of k_0 , only small-amplitude sinusoidal oscillations exist and they finally disappear through the Hopf bifurcation.

Figure 6b gives the dependence of the average number of small-amplitude oscillations on the flow rate. To construct this plot we have assumed that the upper band of points at $[\text{Br}^-]_{\text{max}} > 3 \times 10^{-6} \text{ M}$ corresponds to large-amplitude oscillations, whereas the lower band represents small-amplitude oscillations. Figure 6b illustrates that the average number of small-amplitude oscillations increases with an increase of flow rate. In the general case this dependence is characterized by a “Devil’s staircase” and may be described by a complicated scaling law for the positions of the bifurcation points. However, experiments do not show this “Devil’s staircase”, since the steps of the flow range changes are too coarse, and only the general trends are observed. Comparison of the simulated data presented in Figures 5 and 6 with the experimental results indicates a good correspondence between them. Namely, the experiments and simulations both give similar dependencies of oscillation’s attributes on k_0 : the average number of small-amplitude oscillations and the time intervals between large-amplitude maxima increase with the flow rate.

Modeling of the NO Effect. The NO species may be involved in chemical reactions with any of the bromine-containing species of the BZ reaction, except bromide ions, as well as with the catalyst and the organic compounds. Unfortunately, there is no kinetic data regarding these reactions. Therefore, some estimates and assumptions should be performed in order to select a proper reaction, which is responsible for the effect of NO on the mixed-mode oscillations. Analysis of the literature indicates that reactions between NO and metal ion coordination chemical compounds or organic molecules may not be taken into account since they are sufficiently slow, i.e., a few orders of magnitude less compared to the oxidation of NO by inorganic oxidants.^{25–29} Hypobromous acid is more reactive compared to bromate ions or bromous acid.^{18,30–31} Particularly, the reaction between HOBr and NO is characterized by a higher value of free energy compared to BrO_3^- and HBrO_2 .^{32–33} Taking all these arguments into account, we may consider only the NO oxidation according to the following process:



While there appears no reference to the kinetic parameters of this reaction in the literature, one may assume that the rate of bromide ions production according to (eq 8) is proportional to the concentrations of NO and HOBr in the solution. According to Henry’s law the NO concentration in solution is proportional to the NO concentration in the gas phase. Therefore, the rate of reaction 8 is proportional to the NO concentration in the gas phase. Finally, we obtain the following expression for the bromide ions production according to the reaction 8

$$d[\text{Br}^-]/dt = k_8[\text{HOBr}][\text{NO}] = k_{\text{eff}} P_{\text{NO}} = \nu_8 \quad (\text{R8})$$

where k_8 is the rate constant of reaction 8, $[\text{HOBr}]$ and $[\text{NO}]$ are the concentrations of HOBr and NO in solution, P_{NO} is the partial pressure of NO. We assume that the concentration of HOBr is constant because it is not used as a variable. The concentration of HOBr has been eliminated from the extended kinetic scheme in order to obtain the model presented in Table 2.¹⁶ Taking this into account, the value of k_{eff} is constant and defined as $k_{\text{eff}} = k_8 [\text{HOBr}]_{\text{ss}} K$, where $[\text{HOBr}]_{\text{ss}}$ is a steady-state concentration of HOBr, and K is the Henry constant.

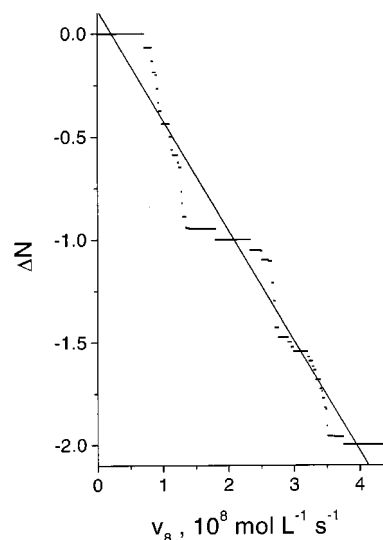


Figure 7. Dependence of ΔN on ν_8 at $k_0 = 1.309 \times 10^{-3} \text{ s}^{-1}$. Simulations are performed according to the model presented in Table 2 and the additional reaction 8.

Expression R8 illustrates that the effect of NO may be considered as an appearance of the additional source for bromide ions production. Finally, the total rate of bromide ions production is given by the following expression:

$$d[\text{Br}^-]/dt = \nu_7 + \nu_6 - \nu_1 - \nu_2 + \nu_8$$

where ν_7 , ν_6 , ν_1 , and ν_2 are the rates of appropriate reactions of the model and ν_8 gives the extra rate of bromide ions production induced by NO species according to reaction 8. The rates for other species of the model (HBrO_2 , BrMA , and M_{ox}) remain the same as for an unperturbed system.

A lack of knowledge regarding explicit values of k_8 and $[\text{HOBr}]_{\text{ss}}$ does not allow us to consider the NO partial pressure as a bifurcation parameter for making a quantitative consideration of the NO effect on mixed-mode regimes. However, the value of ν_8 is proportional to the NO partial pressure. Therefore, the effect of NO on mixed-mode regimes may be described semiquantitatively as a dependence of system behavior on ν_8 .

Our simulations have shown that at any inflow rate the average number of small-amplitude oscillations decreases with an increase of ν_8 , i.e., with an increase of NO concentration in accord with the experimental results. The corresponding bifurcation diagrams are similar to that shown in Figure 6a. Figure 7 gives the dependence of ΔN on ν_8 for the conditions where the unperturbed system ($\nu_8 = 0$) exhibits the LS^3 regime. An increase of ν_8 causes a sequence of period-adding bifurcations leading consequently to LS^2 and LS^1 regimes. Between each two neighboring patterns, LS^i and LS^{i-1} , there is a bunch of more complex patterns. Each of them may be presented as a mixture of LS^i and LS^{i-1} patterns. The dependence shown in Figure 7 is characterized by a “Devil’s staircase” and may be described by a complicated scaling law for the positions of the bifurcation points. However, to make a quantitative correspondence between experimental results and simulations, one may approximate this dependence as a linear one. Analysis of data shown in Figure 7 indicates that linear fit is valid with a regression coefficient of 0.98.

Comparison of data presented in Figures 4a and 7 indicates that there is a good correspondence between experimental results and simulations. The agreement is more pronounced if we consider dependencies of π on k_0 obtained in simulations and

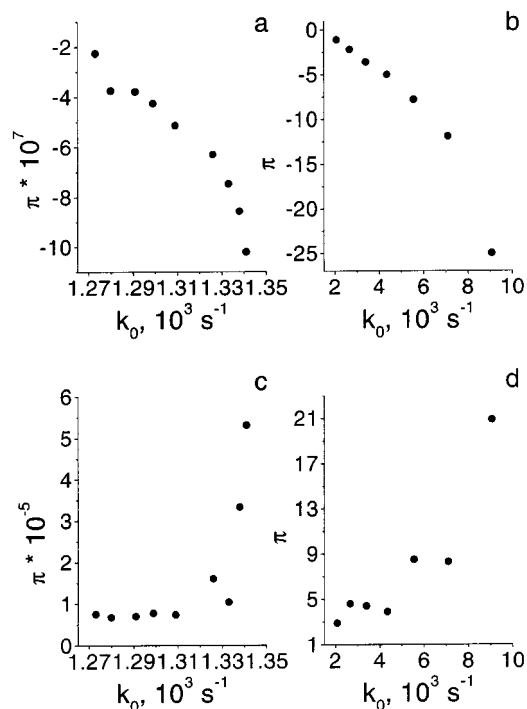
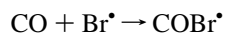


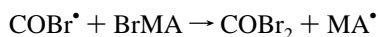
Figure 8. Dependence of π on k_0 obtained in experiments (b,d) and simulations (a,c) for NO (a,b) and CO (c,d). The simulations are performed according to the model presented in Table 2 to which the appropriate reactions, described in the text, were added. The value of π obtained in simulations for NO has been calculated as a slope of the dependence of ΔN on v_8 at a given value of flow rate. For the linear fit the range of v_8 has been taken between zero and value of v_8 that corresponds to the end of the LS¹ regime. The value of π obtained in simulations for CO has been calculated as a slope of the dependence of ΔN on k_9 at a given value of flow rate. For the linear fit the range of k_9 has been taken between zero and value of k_9 that corresponds to the end of the LS⁴⁰ regime.

experiments which are presented in Figures 8, parts a and b. It is clear that the dependence of π on k_0 has the same trend in both cases.

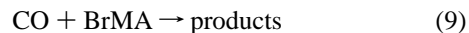
Modeling of the CO Effect. Compared to NO, CO is less reactive. Reactions between carbon monoxide and nonradical species are slower compared to reactions between CO and free radical species.³⁴ Actually, reactions between CO and free radical species give a typical way for the CO conversion. Therefore, for modeling of the CO effect on mixed-mode regimes we may consider only the CO oxidation by radical species that are presented in the BZ reaction, i.e., by various organic radicals, BrO_2^* , and Br^* . Reactions between CO and organic radicals may not be taken into account because they would not affect concentrations of the species of the Györgyi–Field model. Reactions of BrO_2^* are usually characterized by rate constants that are a few orders of magnitude smaller comparing to reactions of Br^* .^{18,35–36} Therefore, as a first step for CO conversion in the BZ reaction, we may consider only the reaction between CO and radicals Br^* :



Next, radicals COBr^* consume the bromomalonic acid:



As a result, the net reaction that describes an effect of CO may be written in the following form:



Therefore, the effect of CO is caused by a consumption of the bromomalonic acid with the rate given by the following expression:

$$d[\text{BrMA}]/dt = -k_{\text{eff}}[\text{CO}][\text{BrMA}] = -k_9[\text{BrMA}] \quad (\text{R9})$$

Following the same arguments that have been presented for the description of the NO effect, k_9 is a constant proportional to the CO partial pressure. Expression (R9) illustrates that the effect of CO may be considered as an appearance of the additional route to bromomalonic acid consumption. Finally, the total rate of bromomalonic acid production is given by the following expression:

$$d[\text{BrMA}]/dt = v_1 + 2v_2 + v_4 - v_6 - v_7 - k_9[\text{BrMA}]$$

where $v_1, v_2, v_4, v_6,$ and v_7 are the rates of appropriate reactions of the model, and the last term gives the extra rate of bromomalonic acid consumption induced by CO species according to reaction 9. The rates for other species of the model ($\text{HBrO}_2, \text{Br}^-,$ and M_{ox}) remain the same as for an unperturbed system.

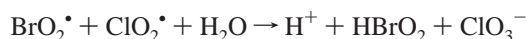
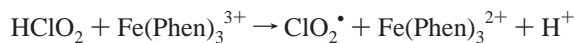
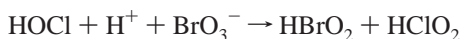
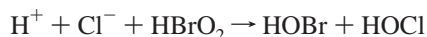
Similar to the analysis of the NO effect, a bifurcation diagram constructed as a dependence of bromide ions maximal concentrations on the k_9 illustrates an effect of CO on mixed-mode oscillations. Our simulations have indicated that the bifurcation diagram is similar to that shown in Figure 6a. We have found that at any value of flow rate an average number of small-amplitude oscillations always increases with an increase of k_9 , i.e., with an increase of the CO concentration in the gas phase. Figure 8c gives the dependence of π on k_0 obtained in simulations for the CO, and Figure 8d gives the same dependence obtained in experiments. These data illustrate that for the effect of CO on mixed-mode regimes we have also obtained a good agreement between experiments and simulations.

Data presented in Figure 8 illustrate that modeling gives the same trend as that observed in experiments for dependence of π on flow rate for NO as well as for CO. For NO both experimental and simulated dependencies are smooth, whereas for CO both of them are scattered. The scattering of points in the case of CO is caused by the following reason. Number of small-amplitude oscillations increases with an increase of the CO concentration. With an increase of N the width of intervals of bifurcation parameter (i.e., gas concentration) with the same mixed-mode regime shrinks resulting in an increase of deviation from linear fit. This leads to scattering of values of π . The scattering is less pronounced in the case of NO because intervals between intervals of bifurcation parameter with the same mixed-mode regime are wider for low values of a number of small-amplitude oscillations.

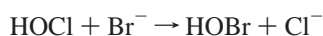
Modeling of the Cl_2 Effect. Contrary to the effect of the CO or NO species on the mixed-mode regimes in the BZ reaction, the effect of Cl_2 is much more complicated. At high flow rates bubbling of Cl_2 induces the $\text{LS}^n \rightarrow \text{LS}^{n-m}$ transitions whereas at low flow rate it induces the $\text{LS}^n \rightarrow \text{LS}^{n+m}$ transitions. Our attempts to give even a semiquantitative explanation to these experiments have failed. Despite the failure, it is worthwhile to describe briefly our efforts. We have assumed that the Cl_2 species primarily disproportionate producing Cl^- and HOCl according to the following equilibrium:



Therefore, the effect of Cl_2 may be considered as an effect of Cl^- and HOCl species which is well-known. Particularly, it has been found that chloride ions may inhibit oscillations in the BZ system.^{37–38} It may be described by the following chemical reactions:³⁹

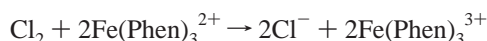


We have also considered an oxidation of bromide ions by HOCl :



$$E = 0.16 \text{ V}$$

and direct oxidation of ferroin by chlorine:



To model the Cl_2 effect on mixed-mode regimes in the same way as it has been performed for NO and CO, we used a steady-state assumption for all chlorine-containing species. This leads to the appearance of additional terms, proportional to partial pressure of chlorine, in velocities for the species of the Györgyi–Field model. We have found that, depending on reactions selected for a consideration, a number of small-amplitude oscillations either increases or decreases with an increase of the partial pressure of Cl_2 . We have not found conditions for the case when the number of small-amplitude oscillations increases at low flow rates and decreases at high flow rates. Possibly this is caused by a necessity to add fifth variable (Cl^- or HOCl) to the Györgyi–Field model. However, such an analysis requires a knowledge of the values of rate constants for appropriate chemical reactions that makes it more complicated and less sophisticated.

5. Discussion

Our studies have indicated that mixed-mode regimes observed in the BZ reaction are sensitive to NO, CO, and Cl_2 . An effect of a given chemical compound on the mixed-mode regime depends strongly on the chemical nature of the compound and the parameters of the BZ reaction. We have illustrated that this effect is caused by chemical reactions between these compounds and species of the BZ reaction. The effect of NO may be accounted for by its oxidation by HOBr . The effect of CO may be attributed to an oxidation of the CO species by radicals present in the BZ reaction and further consumption of bromomalonic acid. Comparison of experimental results and theoretical studies, performed according to these assumptions and is illustrated by Figure 8, indicates that the dependence of the coefficient π on the flow rate has the same trend in simulations and experiments for NO and CO. A good agreement between experimental results and simulations illustrates that the Györgyi–Field model may be considered as a minimal chemically reasonable model that describes properties of mixed-mode regimes observed in the BZ reaction. Contrary to CO or NO, we have failed in our attempts to give a semiquantitative explanation of the effect of the Cl_2 species.

Our experiments show that for the examined gases, namely, NO, CO, and Cl_2 , the data generally fit an empirical straight line $\Delta N = \alpha + \pi \times P$ where P is a partial pressure of a given gas. The magnitude and sign of the coefficient π depends on the chemical nature of the gas as well as on values of control parameters (i.e., flow rate). It seems that the value of α should be zero. The data shown in Figure 4a,b indicate that this holds for NO and CO. However, for Cl_2 the value of α differs significantly from zero as it follows from the data shown in Figure 4c,d. This illustrates that the linear approximation for the dependence of ΔN on the gas partial pressure holds only within some interval of gas concentration. The deviations from linearity are attributed to a “Devil’s staircase”. These “stairs” are not observed experimentally because ranges of change of the bifurcation parameters (flow rate, gas partial pressure) with the same pattern are too small compared to the step of the bifurcation parameter change. Nevertheless, our studies illustrate that linear approximation is fairly good in a certain range of gas concentrations.

The results presented in Figure 8 indicate that magnitude of the coefficient π for NO and CO increases with an increase of flow rate. This is associated with an increase of a number of small-amplitude oscillations in mixed-mode regime if we increase flow rate. Figure 6 illustrates roughly that the intervals of k_0 where a given mixed-mode regime exists shrink with an increase of k_0 , i.e., with an increase of N . Therefore, the higher N requires the smaller changes of control parameter to change the regime. However, this is not the case for Cl_2 . The data presented in Table 1 indicate that magnitude of π for Cl_2 decreases with an increase of k_0 , i.e., with an increase of N . Our theoretical analysis has been based on an assumption that perturbation of the system by a gas does not change the structure of the model. Particularly, the effect of CO and NO has been reduced to an appearance of additional terms in the differential equations that describe the model. In this case we have obtained a good agreement between experiments and simulations, and the results are also in agreement with the assumption that the value of π should increase with an increase of N . The contradiction with this assumption obtained for Cl_2 indicates that a structure of the model should be changed, i.e., one needs a fifth variable to describe the effect of Cl_2 on a mixed-mode regime.

6. Conclusions

In this work we have reported that the dynamical response of nonlinear chemical system is sensitive to the concentration of NO, CO, or Cl_2 . Particularly, an average number of small-amplitude oscillations in a mixed-mode regime observed in the BZ reaction depends linearly on the inflow concentrations of these chemical species. This may be a basis for a construction of a relatively sensitive “detector” which changes a mixed-mode regime under a given perturbation. An operation of such a detector is fairly simple. One should just count the change in the number of small-amplitude oscillations that have been changed by a perturbation of the system. Our results also illustrate that one may obtain a certain level of specificity in the dynamical response of the system to chemical species. Namely, depending on the chemistry of a given species, the number of small-amplitude oscillations either increases or decreases. Moreover, the system response to a given species may be tuned up by an appropriate choice of parameters of the system.

Acknowledgment. The work was supported financially by INTAS Grant INTAS-OPEN-97-1094.

References and Notes

- (1) *Oscillations and travelling waves in chemical systems*; Field, R. J., Burger M., Eds.; Wiley-Interscience: New York, 1985.
- (2) Hudson, J. L.; Hart, M.; Marinko, D. *J. Chem. Phys.* **1999**, *71*, 1601.
- (3) Hudson, J. L.; Mankin, J. C. *J. Chem. Phys.* **1981**, *74*, 6171.
- (4) Maseiko, J.; Swinney, H. L. *J. Chem. Phys.* **1986**, *85*, 6430.
- (5) Scott, S. K. *J. Chem. Phys.* **1991**, *94*, 1134.
- (6) Petrov, V.; Scott, S. K.; Showalter, K. *J. Chem. Phys.* **1992**, *97*, 6191.
- (7) Wang, J.; Sørensen, P. G.; Hynne, F. *J. Phys. Chem.* **1994**, *98*, 725.
- (8) Epstein, I. R.; Showalter, K. *J. Phys. Chem.* **1996**, *100*, 13132.
- (9) Strizhak, P. E.; Kawczyński/Trotman-Dickinson, A. F., et al., Eds.; ski, A. L. *J. Phys. Chem.* **1995**, *99*, 10830.
- (10) Strizhak, P.; Menzinger, M. *J. Chem. Educ.* **1996**, *73*, 868.
- (11) Yatsimirskii, K. B.; Strizhak, P. E.; Ivashchenko, T. S. *Talanta* **1993**, *40*, 1227.
- (12) Strizhak, P. E.; Khavrus, V. O.; Goncharenko, M. M.; Ivashchenko, T. S. *Theor. Exp. Chem.* **1998**, *34*, 153.
- (13) Noszticzius, Z.; McCormick, W. D.; Swinney, H. L. *J. Phys. Chem.* **1987**, *91*, 5129.
- (14) Noszticzius, Z.; McCormick, W. D.; Swinney, H. L. *J. Phys. Chem.* **1989**, *93*, 2796.
- (15) Strizhak, P. E.; Khavrus, V. O. *Talanta* **2000**, *51*, 863.
- (16) Györgyi, L.; Field, R. J. *J. Phys. Chem.* **1991**, *95*, 6594.
- (17) Scott, S. K. *Oscillations, waves, and chaos in chemical kinetics*; Oxford University Press: New York, 1994.
- (18) Györgyi, L.; Turányi, T.; Field, R. J. *J. Phys. Chem.* **1990**, *94*, 7162.
- (19) Györgyi, L.; Rempe, S. L.; Field, R. J. *J. Phys. Chem.* **1991**, *95*, 3159.
- (20) Kawczyński, A. L.; Bar-Eli, K. *J. Phys. Chem.* **1995**, *99*, 16636.
- (21) Kawczyński, A. L.; Bar-Eli, K. *J. Phys. Chem. A* **1997**, *101*, 4592.
- (22) Kawczyński, A. L.; Strizhak, P. E. *J. Chem. Phys.* **2000**, *112*, 6122.
- (23) Kawczyński, A. L.; Khavrus, V. O.; Strizhak, P. E. *Chaos* **2000**, *10*, 299.
- (24) Goryachev, A.; Strizhak, P.; Kapral, R. *J. Chem. Phys.* **1997**, *107*, 2881.
- (25) Laverman, L. E.; Hoshino, M.; Ford, P. C. *J. Am. Chem. Soc.* **1997**, *119*, 12663.
- (26) Reszka, K. J.; Bilski, P.; Chignell, C. F. *J. Am. Chem. Soc.* **1996**, *118*, 8719.
- (27) Akaike, T.; Yoshida, M.; Miyamoto, Y.; Sato, K.; Kohno, M.; Sasamoto, K.; Miyazaki, K.; Ueda, S.; Maeda, H. *Biochemistry* **1993**, *32*, 827.
- (28) Moore, E. G.; Gibson, Q. H. *J. Biol. Chem.* **1976**, *251*, 2788.
- (29) Mayer, B.; Klatt, P.; Werner, E. R.; Schmidt, K. *J. Biol. Chem.* **1995**, *270*, 655.
- (30) Beckwith, R. C.; Margerum, D. W. *Inorg. Chem.* **1997**, *36*, 3754.
- (31) Furman, C. S.; Margerum, D. W. *Inorg. Chem.* **1998**, *37*, 4321.
- (32) *Comprehensive Inorganic Chemistry*; Trotman-Dickinson, A. F., et al., Eds.; Pergamon Press: Oxford (England), 1973; Volume 3.
- (33) Epstein, I. R.; Kustin, K. *J. Phys. Chem.* **1985**, *89*, 2275.
- (34) Ryu, I.; Sonoba, N. *Angew. Chem., Int. Ed. Engl.* **1996**, *35*, 1050.
- (35) Field, R. J.; Raghavan, N. V.; Brummer, J. G. *J. Phys. Chem.* **1982**, *86*, 2443.
- (36) Merenyi, G.; Lind, J. *J. Am. Chem. Soc.* **1994**, *116*, 7872.
- (37) Zhabotinskii, A. M. *Biofizika* **1964**, *9*, 306.
- (38) Janijic, D.; Stroot, P.; Burger, U. *Helv. Chim. Acta* **1974**, *57*, 266.
- (39) Jacobs, S.; Epstein, I. R. *J. Am. Chem. Soc.* **1976**, *98*, 1721.